

INFLUENCE OF THE MAGNETIC CANOPY ON THE DISPERSION RELATION OF WAVES IN THE SOLAR ATMOSPHERE

M. HABERREITER* and W. FINSTERLE

Physikalisch-Meteorologisches Observatorium Davos, Dorfstrasse 33, CH-7260 Davos Dorf, Switzerland (margit.haberreiter@pmodwrc.ch, wolfgang@pmodwrc.ch)

Received ; accepted

Abstract. Observations carried out with the Magneto-Optical Filter at Two Heights (MOTH) experiment show upward traveling waves in magnetic regions with frequencies below the acoustic cut-off. We demonstrate that the dispersion relation of the observed waves show significant differences in magnetic and non-magnetic regions. More importantly, in the low β -regime we do not see the dispersion relation of the field guided slow acoustic mode with a lowered cut-off frequency. Our comparisons with theoretical dispersion relations do not indicate one single wave type for the upward low-frequency wave. From this we conclude that partial mode conversion and transmission takes place.

Keywords: helioseismology; wave propagation; magneto-acoustic waves; radiative transfer

1. Introduction

Recently, the observation and analysis of upward traveling waves in the solar atmosphere has become of great interest, as they are thought to provide a considerable amount to the heating of the chromosphere. Commonly it was understood that only waves with frequencies above the acoustic cut-off frequency, ω_0 , could travel freely in the solar atmosphere, whereas waves with lower frequencies are trapped inside the acoustic cavity of the Sun. However, recent studies by a number of researchers have detected upward traveling waves with frequencies $\omega < \omega_0$.

First, from observations with the Transition Region and Coronal Explorer (TRACE; Handy et al. 1999) De Pontieu et al. (2004) and McIntosh et al. (2006) show that the presence of an inclined solar magnetic field allows low-frequency waves to propagate into the solar chromosphere. The same effect is shown by Jefferies et al. (2006) with data taken with the Magneto-Optical filter at Two Heights (MOTH; Finsterle et al. 2004a) experiment. Furthermore, Vecchio et al. (2007) find low-frequency upward traveling waves in the velocity signal measured simultaneously in Fe I 7090 Å and Ca II 8542 Å with the Interferometric BIdimensional Spectrometer (IBIS; Cavallini 2006).

* current affiliation: Laboratory for Atmospheric and Space Physics, University of Colorado, 1234 Innovation Drive, Boulder, CO, 80303, USA, haberreiter@lasp.colorado.edu

What is the nature of the observed low-frequency waves, i.e. are they the slow acoustic or the fast magnetic waves? De Pontieu et al. (2004), McIntosh and Jefferies (2006) and Jefferies et al. (2006) consider the low-frequency waves in areas with inclined magnetic field to be the field guided slow acoustic waves mode leaking through 'portals' where the inclined magnetic field lowers the acoustic cut-off. Numerical simulations, carried out by Steiner et al. (2007) and Rosenthal et al. (2002) indicate the possibility of mode conversion and transmission, which goes in line with theoretical calculations by Cally (2005, 2006, 2007). From MOTH observations Finsterle et al. (2004b) show that the 'magnetic canopy' (i.e. the $\beta \sim 1$ layer, with $\beta = 8\pi p_g/B^2$, and p_g being the gas pressure and B the magnetic flux density) has a strong influence on the propagation behavior of magnetoacoustic gravity waves.

2. Wave modes

The different wave modes in the solar atmosphere are very well understood from the theoretical point of view, however the determination of the wave modes from the observation remains still a difficult task. The actual wave type depends on the local sound speed c , Alfvén speed a , pressure p , temperature T , magnetic flux density B and field inclination Θ . Generally, the following types of waves can be distinguished (for details see e.g. Rosenthal et al., 2002; Bogdan et al., 2002, 2003; Khomenko & Collados, 2006, Cally, 2005, 2006, 2007; Schunker & Cally, 2006). In high plasma- β regions ($\beta = 8\pi p/B^2$) the fast mode is a longitudinal acoustic wave, and the slow mode is a transverse Alfvén wave. In low plasma- β regions the fast mode is a compressive wave with the gas pressure and the magnetic pressure as restoring force. According to Rosenthal et al. (2002), for high magnetic field strengths, the fast-mode displacement is perpendicular to B irrespective of the propagation direction. For weak magnetic fields, the fast-mode displacement is nearly aligned with the wave vector irrespective of the field direction. In low plasma- β the slow mode is a longitudinal acoustic wave propagating along the magnetic field lines.

Rosenthal et al. (2002) and Bogdan et al. (2002, 2003) showed from 2D numerical MHD simulation that the fast and slow waves undergo coupling at the layer where the plasma- β is of the order of unity. Similarly, Cally (2005, 2007) suggest mode transmission and mode conversion to take place at the layer where the sound speed equals the Alfvén speed. In Cally's terms, mode transmission is the change of a fast acoustic (magnetic) wave to a slow acoustic (magnetic) wave and vice versa. Mode conversion is the change from a fast (slow) acoustic to a fast (slow) magnetic wave and vice versa. In the following we use Cally's notation of mode conversion and transmission. It

is clear that in order to identify the wave type from the observation “it is imperative to determine whether the spectral line or continuum is formed in low or high- β plasma,” (Bogdan et al., 2003). This is pursued in the present paper.

3. Data

The MOTH experiment observed simultaneous Doppler shifts in the K I 7699 Å and Na I 5890 Å lines during a South Pole campaign in the austral summer 2002/03 (Finsterle et al. 2004a) of the full solar disk with a resolution of 3.7 Mm pixel⁻¹. Here we make use of the (455 Mm x 455 Mm 17.8 hr) data cube taken at disk center starting on 2003 January 20, 00:59 UT. Figure 1, panel (a) shows the phase travel time t_{ph} between the K I 7699 Å and Na I 5890 Å observing layers for waves with frequency $\omega=3.0$ mHz. In non-magnetic regions the mean phase travel time is $\bar{t}_{\text{ph}} \approx 0$ (green-blue areas), while the yellow and red pixels indicate upward traveling waves in regions that coincide with enhanced magnetic flux density in the concurrent MDI magnetogram (panel b). Under the assumption of a significant amount of inclined field lines in the magnetic areas, this agrees well with the findings by De Pontieu et al. (2004), McIntosh and Jefferies (2006).

4. Magnetic canopy and formation heights

Following the concept of mode transmission and conversion (Cally, 2007) implies that low-frequency upward traveling waves are only detectable in regions where $\beta=1$ layer is below the formation heights of the spectral lines employed in the MOTH experiment. Otherwise the wave would be evanescent. To test this hypothesis we use magnetic field extrapolations (McIntosh et al. 2001) of the MDI magnetogram in Figure 1b to estimate the plasma- β from the plage model atmosphere structure by Fontenla et al. (2006). The field extrapolations are carried out with respect to the mean observational height of Ni I 6768 Å in the four MDI-filters employed to determine the magnetic flux density. Furthermore, from radiative transfer calculations carried out with COSI (Haberreiter et al. 2008a,b) we determine the formation height of K I 7699 Å and Na I 5890 Å at disk center for the quiet Sun and plage. Note that the formation heights change for different view angles or positions on the solar disk. Here we focus only on plage and leave the sunspots for a later study.

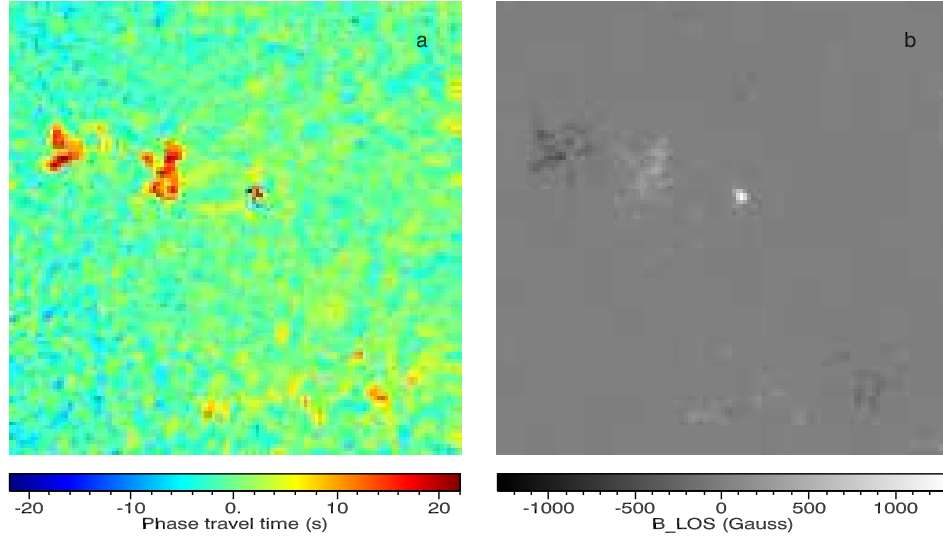


Figure 1. Phase travel time map (455 Mm x 455 Mm at disk center) for waves with frequency $\omega=3.0$ mHz (a) and the concurrent MDI magnetogram (b). The yellow and red pixels indicate upward traveling waves with phase travel times up to 22 s, coinciding with magnetic regions in the MDI magnetogram, whereas $\bar{t}_{ph} \approx 0$ for the non-magnetic areas.

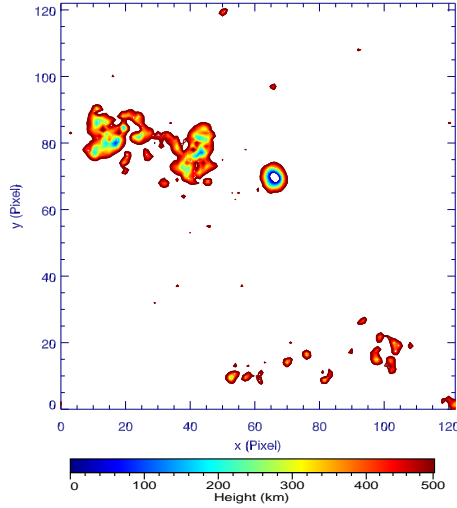


Figure 2. Contours where $\beta=1$ below the Na I 5890 Å formation height in plage. The height scale is with respect to $h(\tau_{500} = 1)$. The areas where the $\beta=1$ layer is below the Na I 5890 Å formation height coincide with areas of higher phase travel time in Figure 1. The white color indicates that the $\beta = 1$ -layer is above the formation height of Na.

Table I. Formation height (km) with respect to $\tau_{500} = 1$ calculated for the quiet Sun and plage for disk center. Also listed are the mean sound speed c at the formation heights and the cut-off frequency ω_0 derived from the atmosphere structures.

area	z_{Na} (km)	z_{K} (km)	Δz (km)	c (km/s)	ω_0 (mHz)
Quiet Sun	530	160	370	6.5	5.6
Plage	490	270	220	7.2	5.0

From $\tau_\lambda = 1$ and the position of the Magneto-Optical Filters (MOFs) in the MOTH instrument we derive the mean observing height of K I 7699 Å and Na I 5890 Å, given in Table I. For a detailed discussion of the MOTH observing heights see Haberreiter et al. (2007). Figure 2 shows the colored contours of the calculated $\beta=1$ layer below the Na I 5890 Å observing height for plage. The red contours indicate where the $\beta=1$ layer coincides with the observational height of Na I 5890 Å (490 km). Toward the center of the active regions the $\beta=1$ layer drops and reaches heights lower than the observational height of K I 7699 Å, $z_{\text{K}} = 270$ km (green to blue contours). The striking congruence of the areas where waves propagate (Figure 1a) and where $\beta=1$ cuts through the MOTH observing layers, in particular the areas where $z_{\beta=1} < z_{\text{K}}$ supports the assumption by Jefferies et al. (2006) that the low-frequency waves propagate only in low- β regions. Moreover, this consistency indicates that the formation heights calculated with COSI from the 1D atmosphere structures are correct.

5. Dispersion relations

Low-frequency traveling waves in the solar atmosphere are generally explained by a lower cut-off frequency due to the inclined magnetic field. According to Campos (1987) the reason is that at high altitudes (i.e. low- β) the acoustic-gravity waves must follow the magnetic field lines, increasing the scale height by the factor $(\cos \Theta)^{-1}$, with Θ being the field inclination to the vertical. Formally, this can also be described with a change of the effective gravitational acceleration $g_{\text{eff}} = g_0 \cos \Theta$ (De Pontieu et al. 2004). A lowering of the acoustic cut-off frequency however implies that the wave should still show the acoustic dispersion relation. To test this hypothesis we compare the group and phase travel times derived from the MOTH data with theoretical values. The fitting of phase travel time t_{ph} and the group travel time t_{gr} is described in detail by Finsterle et al. (2004b) and briefly outlined here. The time series of the K and Na data cubes are first frequency-

filtered with a Gaussian of width $\delta\omega=0.54$ mHz and then cross correlated. The resulting cross-correlation functions are then fitted by least square fits to

$$y(t) = \frac{A^2\delta\omega}{\sqrt{8\pi}} \exp\left[-\frac{\delta\omega^2(t-t_{\text{gr}})^2}{8}\right] \cos[\omega(t-t_{\text{ph}})] \quad (1)$$

whereby the t_{ph} , t_{gr} , the amplitude A , the central frequency ω , and the width of the Gaussian filter $\delta\omega$ are the fitted variables. In Figure 3 the fits for t_{gr} (thin lines) and t_{ph} (thick lines) are shown for different height intervals of the $\beta = 1$ -layer ($z_{\beta=1}$) with respect to the formation height of Na (z_{Na}) and K (z_{K}): i) $z_{\beta=1} > z_{\text{Na}}$ (solid lines), ii) $z_{\text{Na}} > z_{\beta=1} > z_{\text{K}}$ (dotted lines) and iii) $z_{\beta=1} < z_{\text{K}}$ (dashed lines). The corresponding 1σ -error bars of the travel time fits are shown in Figure 4.

In Figure 3 we find the dispersion relation of acoustic gravity waves ($\omega_0 \sim 5.4$ mHz) for the heights where the $\beta = 1$ -layer is higher than z_{Na} (solid lines), confirming the results of Finsterle et al. (2004b). For $z_{\beta=1} < z_{\text{K}}$ (dashed lines) we find traveling waves at low frequencies ($\omega \leq 5$ mHz) with a mean phase travel time of 8.6 s. The intermediate range ($z_{\text{Na}} > z_{\beta=1} > z_{\text{K}}$) shows the transition stage between the two regimes. For this analysis we considered areas with magnetic flux density up to $B = 500$ G. The mean magnetic flux density for the different height intervals are $\bar{B}=7.7$ G ($z_{\beta=1} > z_{\text{Na}}$), $\bar{B}=47$ G ($z_{\text{Na}} > z_{\beta=1} > z_{\text{K}}$), and $\bar{B}=218$ G ($z_{\beta=1} < z_{\text{K}}$). Note that as the filling factor for plage regions is considered to be smaller than unity, following, at some areas below the instrumental resolution the 'real' magnetic flux density is expected to have higher values than \bar{B} .

5.1. ACOUSTIC WAVE ($\beta > 1$)

For the fast acoustic (fa) wave we use the dispersion relation

$$\omega^2 = c^2 k^2 + \omega_0^2, \quad (2)$$

going back to Bel and Leroy (1977), with c being the sound speed, ($k = \alpha + i\beta$) the complex wave vector and ω_0 the cut-off frequency. Using $k = \pm\sqrt{\omega^2 - \omega_0^2}/c$ we get the phase velocity:

$$v_{\text{ph,fa}} = \frac{\omega}{\pm k} = \pm \frac{c}{\sqrt{1 - \left(\frac{\omega_0}{\omega}\right)^2}} \quad (3)$$

Furthermore, using $\omega = \pm\sqrt{c^2 k^2 + \omega_0^2}$ we get the group velocity as:

$$v_{\text{gr,fa}} = \pm \frac{d\omega}{dk} = \pm \frac{c^2 k}{\sqrt{c^2 k^2 + \omega_0^2}} = \pm \frac{c^2 k}{\omega} = \pm \frac{c^2}{v_{\text{ph}}} = \pm c \sqrt{1 - \left(\frac{\omega_0}{\omega}\right)^2} \quad (4)$$

For $\omega > \omega_0$, $k = \alpha$ and $\beta = 0$, while for $\omega < \omega_0$, k is imaginary ($k = i\beta$), meaning it denotes the evanescent wave, i.e. the wave varies sinusoidally in time, but exponentially in space. In the latter case $\alpha = 0$, $v_{\text{ph}} = \infty$, and $v_{\text{gr}} = 0$. With $t_{\text{ph}} = \Delta z/v_{\text{ph}}$ and $t_{\text{gr}} = \Delta z/v_{\text{gr}}$ it follows that for the evanescent wave we expect $t_{\text{ph}} = 0$, and $t_{\text{gr}} = \infty$. However, as it is impossible to observe an infinite group travel time, we set the theoretical group travel times for the evanescent wave to zero. This is justified by the fact that in the case of the evanescent wave the whole solar atmosphere oscillates in phase, i.e. there is no detectable phase lag between different layers in the atmosphere. As we will see later, this approach agrees well with the observed dispersion relation in non-magnetic regions. Note that evanescent waves do not transmit energy vertically (see e.g. Leibacher and Stein, 1981).

The acoustic cut-off frequency $\omega_0 = \gamma g/4\pi c$ is calculated from the latest solar atmosphere structures for the quiet Sun (Fontenla et al. 2007) and plage (Fontenla et al. 2006). Furthermore, $\gamma=5/3$ is the ratio of the specific heats, $g=274\text{ms}^{-2}$ the gravitational acceleration, $c = \sqrt{\gamma p/\rho}$ the sound speed, p and ρ the depth dependent pressure and density. Note that this is only one of several possible representations of the acoustic cut-off frequency in the quiet Sun (Schmitz and Fleck 1998).

5.2. MAGNETIC WAVES ($\beta < 1$)

Let us now discuss the dispersion relation of upward traveling wave modes that can occur after mode transmission or conversion, i.e. the field guided slow acoustic mode and the fast magnetic mode. The slow acoustic mode is understood to be 'leaking' through magnetic regions by the lowering of the acoustic cut-off frequency in magnetic regions (see Bel and Leroy, 1977; Campos, 1987; Cally, 2006; De Pontieu et al., 2004). Here we account for the lowering of the acoustic cut-off frequency following De Pontieu (2004) and Campos (1987, Eq. 209a):

$$\omega^2 = c^2 k^2 + \omega_{\text{eff}}^2, \quad (5)$$

with $\omega_{\text{eff}} = \omega_0 \cos \Theta$, and Θ being the field inclination derived from the magnetic field extrapolation. Following the above outline for the acoustic wave, we get the phase and group velocity $v_{\text{ph,sa}}$ and $v_{\text{gr,sa}}$ for the field guided slow acoustic (sa) wave mode as:

$$v_{\text{ph,sa}} = \frac{c}{\sqrt{1 - \left(\frac{\omega_{\text{eff}}}{\omega}\right)^2}} \quad (6)$$

$$v_{\text{gr,sa}} = c \sqrt{1 - \left(\frac{\omega_{\text{eff}}}{\omega}\right)^2}. \quad (7)$$

Finally, we derive the dispersion relation of the fast magnetic wave. It is calculated using the dispersion relation by Cally (2006), Eq. (1). Under the assumption of vertically upward traveling waves, i.e. $k_x=0$, their equation simplifies to:

$$\omega^4 - (a^2 + c^2)k^2\omega^2 + a^2c^2k^4 \cos^2 \Theta - (\omega^2 - a^2k^2 \cos^2 \Theta)\omega_0 = 0. \quad (8)$$

From Eq. 8 we derive the phase and group velocity as follows:

$$v_{\text{ph}} = \frac{\omega}{\sqrt{\frac{-b_1 + \sqrt{b_1^2 - 4a_1c_1}}{2a_1}}}, \quad (9)$$

$$v_{\text{gr}} = \frac{1}{4\omega} \left(2(a^2 + c^2)k + \frac{a_2k^3 + b_2k}{\sqrt{a_2k^4 + b_2k^2 + \omega_0^4}} \right) \quad (10)$$

The detailed steps to derive the equations are given in the Appendix. Note that as we consider upward propagating waves, in the following we only consider the positive real parts of complex k and ω . We are aware that the assumption of vertically upward traveling waves in a approximation that is of course not exclusively the case on the Sun.

6. Results

In the following we compare the travel times derived from the observations with the theoretical travel times as outlined above. The theoretical travel times are convolved with the same Gaussian frequency filter as used for the frequency filtering of the MOTH data ($\delta\omega = 0.54$ mHz). Figure 4 compares the observed travel times with the group and phase travel times, calculated as $t_{\text{ph}}(\omega) = \Delta z/v_{\text{ph}}(\omega)$, and $t_{\text{gr}}(\omega) = \Delta z/v_{\text{gr}}(\omega)$ for different regimes in the solar atmosphere. Panel (a) compares the observed travel times for $z_{\beta=1} > z_{\text{Na}}$ with the theoretical values calculated with $\Delta z=370$ km, $c=6.5$ km/s, $\omega_0 = 5.6$ mHz (see Table 1) and no field inclination ($\Theta = 0^\circ$). The theoretical curve represents the observed dispersion relation quite well. For the intermediate β -regime (panel b) we calculate the dispersion relation using $\Delta z=220$ km, $c=7.2$ km, and $\omega_0 = 5.0$ mHz for plage, and a lowered cut-off frequency with $\Theta = 30^\circ$ (dashed lines). We find that the fitted t_{gr} shows a substantially different behavior than the theoretical t_{gr} . In particular, a cut-off frequency is not visible in the travel time fits from the observation. Therefore, we conclude that, while passing through the magnetic canopy, the acoustic nature of the wave is not detectable anymore.

Finally, let's consider the fitted group and phase travel times for $z_{\beta=1} < z_K$. From the field extrapolations we get a mean field inclination of $\Theta =$

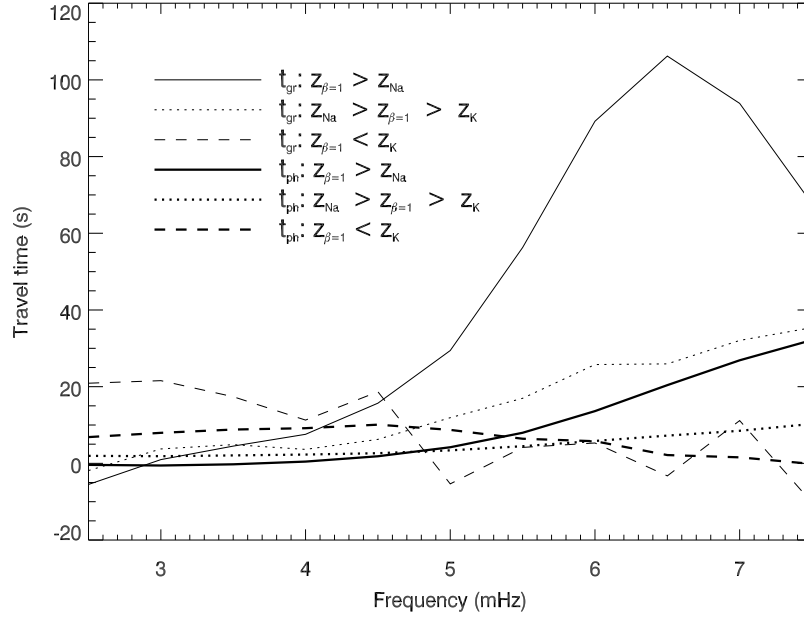


Figure 3. Group and phase travel time (thin and thick lines) derived from the MOTH observations as a function of frequency for different height intervals: $z_{\beta=1} > z_{\text{Na}}$ (solid), $z_{\text{Na}} > z_{\beta=1} > z_K$ (dotted) and $z_{\beta=1} < z_K$ (dashed). For $z_{\beta=1} > z_{\text{Na}}$ we find the dispersion relation as expected for an acoustic gravity wave with a cut-off frequency $\omega_0 \simeq 5.4$ mHz. For $z_{\text{Na}} > z_{\beta=1} > z_K$ the dispersion relation flattens. Finally, for $z_{\beta=1} > z_{\text{Na}}$ we find positive travel times between 2.5 to 5 mHz, and in particular a similar behavior for the group and phase travel time.

68.7°. Panel (c) and (d) shows the fitted travel times together with theoretical values as given in Eq. 11 and 10 using $\Delta z = 220$ km, $c = 7.2$ km, $a = 8.9$ km, and $\omega_0 = 5.0$ mHz and the field inclinations $\Theta = 30^\circ$ (dashed lines) and $\Theta = 70^\circ$ (dashed-dotted lines). In both cases the theoretical travel times are higher than the travel times derived from the observation.. The theoretical values for the group travel times for the fast magnetoacoustic wave with a field inclination of $\Theta = 70^\circ$ is just at the limit of the error bars. This could indicate that we indeed observe the fast magnetoacoustic wave. However the theoretical values of the phase travel time is considerably overestimated.

One reason why the theoretical travel times are larger than the observed values might be that we underestimate the Alfvén due to an underestimation of the magnetic flux density derived from the MDI. As the filling factor for

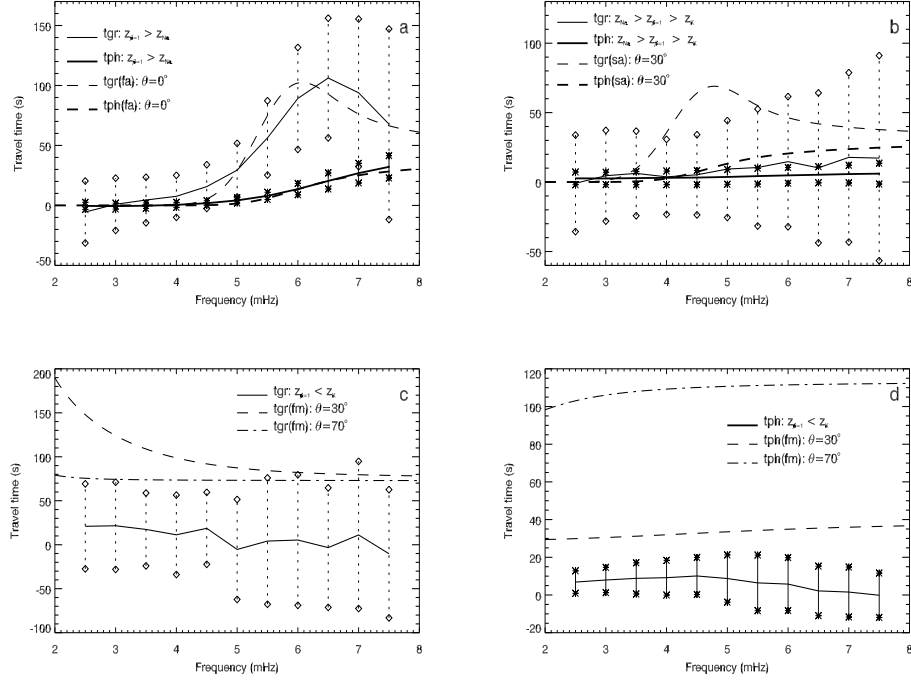


Figure 4. Panel (a) gives the 1σ -error bars for the fitted group (thin line, diamonds) and phase travel times (thick line, stars) for $z_{\beta=1} > z_{Na}$. Also shown are the theoretical travel times t_{gr} and t_{ph} for an acoustic gravity wave with a cut-off frequency $\omega_0 = 5.6$ mHz, which agrees well with the observed travel times. Panel (b) shows the same for $z_{Na} > z_{\beta=1} > z_K$ together with the theoretical dispersion relation based on a lowered cut-off frequency $\omega_{eff} = \omega_0 \cos \Theta$, where $\Theta = 30^\circ$ and $\omega_0 = 5.0$ mHz. Finally, the error bars for the fitted t_{gr} and t_{ph} for $z_{\beta=1} < z_K$ are given in panel (c) and (d) respectively together with the theoretical travel times for $\Theta = 30^\circ$ and $\Theta = 70^\circ$. Please note the different scale in each panel.

the magnetic field of an MDI pixel is less than unity, stronger field strength are most likely to occur at a scale not resolved with the MDI instrument.

7. Discussion

Let us first discuss the significant change of the dispersion relation seen in Figure 4 panel (a) and (b). As the observation heights of Na and K are very close to the $\beta=1$ layer, we might not be able to see a pure slow acoustic wave with a lowered cut-off frequency, but a mixture of wave types, i.e. the slow acoustic and the fast magnetic. Nevertheless, it is striking that the acoustic

dispersion relations seen in the high- β regime vanishes immediately when the observing heights are close to the magnetic canopy.

Furthermore, as the gas and magnetic pressure are of approximately equal amplitude, i.e. the magnetic field is weak, it is possible that the acoustic wave coming from below not only causes longitudinal pressure and velocity fluctuations along the field lines, but also distort the magnetic field lines along the wave vector (see Rosenthal et al., 2002). The combination of these processes might lead to a loss of the acoustic signature in the observations.

One might expect to see the pure slow acoustic wave if we could discriminate waves propagating upward under an angle parallel to the magnetic field. In this case the acoustic wave can not distort the magnetic field lines. Holography, as carried out by Schunker and Cally (2008) for vertically upward traveling waves would be the right tool to select the appropriate incoming waves. In this way we might be able to analyze the dispersion relation of an 'ideal' slow acoustic wave.

The slight decrease of the travel times for frequencies higher than 5 mHz also needs further investigation. Muglach et al. (2005) conclude from MDI and TRACE observations that if the $\beta \sim 1$ layer is below the formation height of the TRACE intensity, the intensity power in the layers above decreases, which they associate with wave reflection. Numerical calculations carried out by Rosenthal et al. (2002) show that wave reflection of high frequency waves (in their case $\omega = 42$ mHz) occurs at the $\beta = 1$ -layer. In the regions above the reflecting surface the wave is still present as an evanescent tail. This could explain the vanishing travel times in the high frequency regime. However, only detailed 3D MHD simulations including realistic density and temperature stratifications can help to fully understand these phenomena.

8. Conclusion

From MOTH observation we show that in magnetic regions low-frequency waves can escape the solar acoustic cavity and propagate upwards between the K I 7699 Å and Na I observing layers. Furthermore, evidence is given that the observed low-frequency waves originate in deep layers as acoustic ($\beta > 1$) and clearly change their characteristics while passing through the magnetic canopy into the low- β regime. In particular, we do not see any evidence for a lowered cut-off frequency in low- β regions. The reason for this could be that when looking at the layer where mode transmission and mode conversion occurs, we actually see a superposition of different wave types. Furthermore, the theoretical travel times predicted from the dispersion relation of a vertically upward propagating fast magnetic wave are higher than the travel times derived from the observations for the low- β

regime. Nevertheless, the theoretical group travel times for the fast magnetic wave gives some indication that it is rather the fast magnetic than the slow acoustic wave that is observed.

We conclude that in order to clearly distinguish various wave types in the solar atmosphere the observational heights have to be clearly separated in the very high and low- β -regimes. It is essential to know to which extent the waves convert and transmit into the slow magnetic and fast acoustic wave, as the different wave types are expected to deposit their energy in different heights of the solar atmosphere.

Acknowledgements

The authors are very grateful to Charles Lindsey for helpful comments and to S. McIntosh for providing us the code to perform the magnetic field extrapolations. MDI data courtesy of the SOHO/MDI Consortium. SOHO is a project of international cooperation between ESA and NASA. The MOTH experiment was funded by award OPP-0087541 from the National Science Foundation (NSF). During this work MH was supported by the Swiss National Science Foundation under grant 200020-109420.

References

- Bel, N. & Leroy, B.: 1977, *Astron. Astrophys.* **55**, 239.
- Bogdan, T. J., Rosenthal, C. S., Carlsson, M., et al. 2002, *Astronomische Nachrichten* **323**, 196.
- Bogdan, T. J., Carlsson, M., Hansteen, V. H., et al. 2003, *Astrophys. J.* **599**, 626.
- Cally, P. S.: 2005, *Mon. Not. R. Astron. Soc.* **358**, 353.
- Cally, P. S.: 2006, *Phil. Trans. R. Soc. A* **364**, 333.
- Cally, P. S.: 2007, *Astronomische Nachrichten* **328**, 286.
- Campos, L. M. B. C.: 1987, *Rev. of Mod. Phys.* **59**, 363.
- Cavallini, F.: 2006, *Solar Phys.* **236**, 415.
- De Pontieu, B. and Erdélyi, R. and James, S. P.: 2004, *Nature* **430**, 536.
- Finsterle, W., Jefferies, S. M., Cacciani, A., Rapex, P., Giebink, C., Knox, A., Dimartino, V.: 2004a, *Solar Phys.* **220**, 317.
- Finsterle, W., Jefferies, S. M., Cacciani, A., Rapex, P., and McIntosh, S. W.: 2004b, *Astrophys. J.* **613**, L185.
- Fontenla, J.M., Avrett E., Thuillier G., and Harder J.: 2006, *Astrophys. J.* **639**, 441.
- , J. M., Balasubramaniam, K. S. and Harder, J.: 2007, *Astrophys. J.* **667**, 1243.
- Haberreiter, M., Schmutz, W., and Hubeny, I.: 2008a, *Astron. Astrophys.* **492**, 833.
- Haberreiter, M., Schmutz, W., and Kosovichev, A.G.: 2008b, *Astrophys. J.* **675**, L53.
- Haberreiter, M., Finsterle, W., and Jefferies, S.M.: 2007, *Astronomische Nachrichten* **328**, 211.
- Handy, B. N. et al.: 1999, *Solar Phys.* **187**, 229.
- Jefferies, S. M., McIntosh, S. W., Armstrong, J. D., et al.: 2006, *Astrophys. J.* **648**, L151.

- Khomenko, E. and Collados, M.: 2006, *Astrophys. J.* **653**, 739.
- Leibacher, J. W. and Stein, R. F.: 1981, in S. Jordan (ed.), *The Sun as a Star*, NASA SP-450, p. 263
- McIntosh, S. W. and Jefferies, S. M.: 2006, *Astrophys. J.* **647**, L77.
- McIntosh, S. W., Bogdan, T. J., Cally, P. S., Carlsson, M., Hansteen, V. H., Judge, P. G., Lites, B. W., Peter, H. Rosenthal, C. S., Tarbell, T. D.: 2001, *Astrophys. J.* **548**, L237.
- Muglach, K., Hofmann, A., and Staude, J.: 2005, *Astron. Astrophys.* **437**, 1055.
- Rosenthal, C. S., et al.: 2002, *Astrophys. J.* **564**, 508.
- Schmitz, F. and Fleck, B.: 1998, *Astron. Astrophys.* **337**, 487.
- Schunker, H. and Cally, P. S.: 2006, *Mon. Not. R. Astron. Soc.* **372**, 551.
- Schunker, H. and Braun, D. C. and Lindsey, C. and Cally, P. S.: 2008, *Solar Phys.* **251**, 341.
- Steiner, O., Vigeesh, G., Krieger, L., Wedemeyer-Böhm, S., Schaffenberger, W., and Freytag, B.: 2007, *Astronomical Notes* **328**, 323.
- Vecchio, A., Cauzzi, G., Reardon, K. P., Janssen, K., and Rimmele, T.: 2007, *Astron. Astrophys.* **461**, L1.

Appendix

For the fast magnetic (fm) wave ($\beta < 1$), we get the positive upward traveling phase velocity $v_{\text{ph}} = \omega/k$ using

$$k = \pm \sqrt{\frac{-b_1 + \sqrt{b_1^2 - 4a_1c_1}}{2a_1}}, \quad (11)$$

as

$$v_{\text{ph}} = \frac{\omega}{\sqrt{\frac{-b_1 + \sqrt{b_1^2 - 4a_1c_1}}{2a_1}}}, \quad (12)$$

where

$$a_1 = a^2 c^2 \cos^2 \Theta \quad (13)$$

$$b_1 = -(a^2 + c^2)\omega^2 - a^2 \cos^2 \Theta \omega_0^2 \quad (14)$$

$$c_1 = \omega^4 - \omega^2 \omega_0^2 \quad (15)$$

Furthermore, using

$$\omega = \sqrt{((a^2 + c^2)k^2 + \omega_0^2 + \sqrt{a_2 k^4 + b_2 k^2 + \omega_0^4})/2} \quad (16)$$

the group velocity, calculated as $d\omega/dk$, is

$$v_{\text{gr}} = \frac{1}{4\omega} \left(2(a^2 + c^2)k + \frac{a_2 k^3 + b_2 k}{\sqrt{a_2 k^4 + b_2 k^2 + \omega_0^4}} \right) \quad (17)$$

with

$$a_2 = (a^2 + c^2)^2 - 4a^2 c^2 \cos^2 \Theta \quad (18)$$

$$b_2 = 2(a^2 + c^2)\omega_0^2 - 4a^2 \cos^2 \Theta \omega_0^2 \quad (19)$$

